JOURNAL OF SOLID STATE CHEMISTRY 137, 261–275 (1998)
ARTICLE NO. SC977732

An *ab Initio* Hartree–Fock Study of the Energies of Mixing of MnO–NiO, MgO–MnO, and CaO–MnO Solid Solutions

Markus Königstein,[1] Furio Corà, and C. Richard A. Catlow

Davy Faraday Research Laboratory, The Royal Institution of Great Britain, 21 Albemarle Street, London W1X 4BS, United Kingdom

Received July 7, 1997; in revised form December 2, 1997; accepted December 5, 1997

We have calculated the energies of mixing of the rock salt structure solid solutions MnO–NiO, MgO–MnO, and CaO–MnO using periodic *ab initio* Hartree–Fock Hamiltonians; *a posteriori* corrections for electron correlation derived from density-functional theory have also been evaluated. The agreement of the correlation-corrected values with available experimental data is very good. Magnetic interactions in the solid are reproduced correctly, but their neglect does not influence strongly the calculated mixing energy. Atomic relaxation, however, has an important effect on the calculated energetics. Comparing the electronic distribution in the pure oxides and the solid solutions, we find neither induced spin polarization on the oxygen ions nor electronic relaxation in the three mixed systems. Additionally, we performed atomistic lattice simulations based on interatomic potentials, which in the case of the MnO–NiO and CaO–MnO solid solutions predict energies of mixing that are significantly high compared with experiment. By fitting to our *ab initio* data we derived a new set of potentials, which reproduce experimental results more accurately. Finally, we calculated the temperature dependence of the energy of mixing for MgO–MnO by performing Gibbs free energy minimizations at different temperatures up to 1000 K. The results indicate a negligible temperature dependence of the calculated energies of mixing.

1. INTRODUCTION

The knowledge of accurate thermodynamic data for the solid solutions of binary oxides is a problem of importance, for instance in the development of improved high-temperature ceramics and in heterogeneous catalysts. Despite more than 30 years of research in this field, accurate thermodynamic data for solid solutions, even for simple rock salt structure oxides, are rare, owing mainly to experimental difficulties in the measurement of small quantities with sufficient accuracy (the experimental enthalpies of mixing are usually less than 10 kJ/mol). The agreement between different available experimental data is often poor: if we consider for example the case of CaO–MnO solid solutions, the published values (1, 2) differ by a factor of more than 2.5. Because of these experimental difficulties in determining the enthalpies of mixing, theoretical models have been commonly used for their prediction. The measured data in these theoretical studies are often represented by regular solution models (excess entropy $\Delta S_{mix} = 0$, $\Delta H_{mix} \neq 0$) or parameterized from ionic size considerations (3, 4). In a more sophisticated study Burdett and Nguyen (5) calculated the energies of mixing of metal oxide solid solutions via a tight-binding Hamiltonian. However, their predicted mixing energies for the 50% solid solutions $Mg_{0.5}M_{0.5}O$ (M = Ca, Mn, Fe, Co, Ni) differ by a factor of between two and four from the available experimental data.

The growth of computer power in recent years and the advances in the computational procedures now allow us to perform *ab initio* calculations of the mixing energies, without using experimentally derived parameters. Thus, the energies of mixing of MgO–MnO and MgO–NiO were recently calculated using *ab initio* periodic Hartree–Fock methods (6). The results are encouraging, especially as the calculations predicted correctly the experimentally observed negative deviations from ideality in the MgO–NiO system, although a discrepancy of a factor of more than two remained between the absolute value of calculated and experimental data. This disagreement may be due to the approximations adopted in this study, in particular the neglect of the relaxation of oxygen ions. Furthermore, these calculations assume the high-spin ferromagnetic state for the solid solution, although from comparison with the magnetic ordering of the pure oxides, we would expect that the high-spin antiferromagnetic state should be more stable. The aim of the current work is to calculate more accurate thermodynamic data for the MnO–NiO, MgO–MnO, and CaO–MnO systems by removing these simplifications. We show that the agreement with experimental data is in this case considerably improved and that accurate *ab initio* calculations can therefore play a valuable role in predicting energies of mixing in systems where thermodynamic data

[1] To whom correspondence shoud be addressed.

0022-4596/98 $25.00

are not yet available or where the agreement with experimental data is unsatisfactory.

This paper is organized as follows: in Section 2 we describe the methods and computational details used in the present investigation. In Section 3 we discuss the results of our calculations: first we comment on the equilibrium lattice constants of the mixed crystals; secondly we report the mixing energies of the solid solutions, calculated using both quantum mechanical techniques and atomistic lattice simulations based on interatomic potentials, subsequently referred to as atomistic simulations. Thirdly we discuss in more detail the mixing energies based on atomistic simulations and compare the results obtained with previously published potential models and a newly derived model which has been fitted to our quantum mechanical calculations. Finally, we comment on the electronic structure of the mixed crystals.

2. METHODOLOGY

2.1. Geometry Definitions for the Solid Solutions

We have studied the binary solid solutions $M_xM'_{1-x}O$ of MnO with three other rock salt structured oxides—NiO, MgO, and CaO—and with the compositions $x = 0.125$, 0.25, 0.5, 0.75, and 0.875. In our calculations the model adopted to represent the bulk materials is based on periodic boundary conditions. Solid solutions of different compositions can in this case be obtained by creating a supercell of the host oxide MO and successively replacing the cation M of the host system by a second cation M' to give the desired stoichiometry.

In our quantum mechanical, Hartree–Fock calculations we represented the ferromagnetic MgO–MnO and CaO–MnO and the ferrimagnetic MnO–NiO mixtures using the following supercells: for the 12.5% (and 87.5%) solid solutions we used 16-ion supercells of the type MM'_7O_8 and for the 50% solid solutions the 4-ion rhombohedral double unit cell $MM'O_2$. Furthermore, for the 25% (75%) solid solutions we must distinguish between the unrelaxed case, in which all internal coordinates were kept at their regular cubic positions, and the relaxed case, where this constraint was removed: in the unrelaxed case the solid solutions were represented through the 8-ion cell of the composition MM'_3O_4; in the relaxed case we used 16-ion supercells of the type $M_2M'_6O_8$, in which the two metal ions M were placed along the [110] direction. In the 8-ion cell MM'_3O_4 all oxygens in fact have symmetry-unique coordinates, and this cell does not allow the relaxation of the oxygen ions to be taken into account. Finally, for the antiferrimagnetic solid solutions of MnO–NiO, calculations were performed on the 16-ion supercells of the compositions $M_4M'_4O_8$ (50% mixture), $M_2M'_6O_8$ (25 and 75% mixtures) and MM'_7O_8 (12.5 and 87.5% mixtures). In the $M_2M'_6O_8$ supercells, the two metal ions M were again placed along the [110] direction, while in the $M_4M'_4O_8$ supercells, the four metal ions M were placed at the positions with the fractional coordinates (0.0, 0.0, 0.0), (0.0, 0.0, 0.5), (0.0, 0.5, 0.0) and (0.0, 0.5, 0.5) [the coordinates refer to the $2 \times 2 \times 2$ expansion of the primitive unit cell]. The spins in all the supercells for the antiferrimagnetic solid solutions have been aligned in ferrimagnetic (111) sheets, with adjacent sheets having antiparallel spin. This arrangement corresponds to the correct antiferromagnetic spin setting in low-temperature antiferromagnetic MnO and NiO and is generally referred to as the AF_2 spin arrangement.

We note that the Hartree–Fock Hamiltonian employed reproduces the correct site symmetry of the crystal field for all the supercells in our study. Splitting of the valence d levels for the Mn and Ni ions is therefore correctly reproduced as a function of the crystalline environment of the ions.

The supercells employed in the atomistic simulations study were the same as in the relaxed ferromagnetic and ferrimagnetic Hartree–Fock calculations, although, obviously, magnetic interactions are not included explicitly in the interatomic potentials employed.

2.2. Hartree–Fock Calculations

The computational model that we have used in our quantum mechanical calculations is based on periodic boundary conditions at the *ab initio* Hartree–Fock level of approximation, as implemented in the CRYSTAL code (7, 8). The open-shell solution of the magnetic oxides MnO and NiO has been represented via an unrestricted Hartree–Fock (UHF) treatment of the spin-dependent part of the wave function.

In CRYSTAL, the wave function of the solid is described in terms of crystalline orbitals; these are obtained as linear combinations of localized functions, or atomic orbitals (LCAO method), associated with the atomic positions. The basis sets have been derived from previous studies on the pure oxides MgO (9), CaO (10), MnO, and NiO (11) (the oxygen basis set is from ref 11 using the exponents of 0.500 and 0.191 $bohr^{-2}$ for the 3*sp* and 4*sp* shells) and correspond to a split-valence, triple-ζ-quality, basis set for the *sp* atomic orbitals, while the *d* atomic orbitals of Mn and Ni are described with a double-ζ basis set; a set of single-ζ-polarization functions was also included for Ca. The properties of the pure oxides were correctly reproduced with the above Hamiltonian and basis functions.

Numerical approximations need to be introduced in the implementation of the HF equations for an infinite system. In the CRYSTAL code, the accuracy of direct space summations for the infinite Coloumb and exchange series is controlled by a set of "cutoff" tolerances (see refs 7 and 8 for more details). We used high values (6, 8, 6, 7, 14), which reduce numerical inaccuracies to a minimum.

Reciprocal space integration was performed by sampling the first Brillouin zone at a regular array of $8 \times 8 \times 8$ k-points for the pure oxides; the irreducible part of the first Brillouin zone includes 29 k-points for the nonmagnetic and the ferromagnetic oxides and 65 k-points for the antiferromagnetic oxides. To obtain the same accuracy in the mixed systems, the sampling has been scaled according to the unit cell dimensions. The chosen sampling ensures convergence of the results in the reciprocal space integrations.

Finally, in the following sections, HF results have been corrected to estimate the effect of electron correlation; having calculated the HF energy and wave function, the correlation correction to the energy is evaluated *a posteriori* with a density functional of the Hartree–Fock equilibrium density, according to the generalized gradient approximation (GGA) scheme proposed by Perdew *et al.* (12, 13). No correction has, however, been attempted for the HF wave function. We consider that the mixing energies, which have been obtained from the Hartree–Fock results and which have been corrected *a posteriori* for electron correlation, are the most reliable provided by our theoretical investigation, and we expect therefore that they should also give the best agreement with experiment.

2.3. Atomistic Simulations

Atomistic lattice simulations based on interatomic potentials have long been a standard technique in computational chemistry; the theoretical background has been extensively described previously as in, for example, ref 14. All our calculations were performed with the computer code GULP (15, 16), using interatomic short-range Buckingham potentials to represent both the M–O and O–O interactions and the shell model to represent the ion polarizability. We have taken the O–O parameters from Catlow (17) (employing a core–shell spring constant of 53.9 eV/Å^2) and the M–O parameters from Lewis and Catlow (18). All the calculations based on interatomic potentials allowed the simultaneous relaxation of the cell parameters and of all the internal coordinates.

The majority of the calculations were based on lattice energy minimizations. However, to study the temperature dependence of the energy of mixing, we also performed calculations on the MgO–MnO system at 0, 500, and 1000 K; in the latter case we minimized the Gibbs free energy at the specified temperature using the approximation that the principal effect of temperature is to vary the size of the unit-cell, i.e., the quasi-harmonic approximation. The Gibbs free energy is related to the Helmholz free energy by the expression

$$G = A + pV,$$

whereby G is the Gibbs free energy, A is the Helmholz free energy, V is the unit cell volume, and p is the pressure, which has two components—any external applied pressure, p_{ext}, and the internal, phonon pressure, p_{int}, arising from the lattice vibrations:

$$p = p_{\text{ext}} - p_{\text{int}}.$$

The phonon pressure is given by

$$p_{\text{int}} = -\partial A/\partial V.$$

To calculate the Gibbs free energy, it is therefore necessary to calculate the Helmholz free energy and its derivative with respect to the unit cell volume. After minimizing the internal energy of the structure with respect to all unit cell parameters and internal degrees of freedom, the GULP code calculates, for the optimized structure, second derivatives of the energy with respect to both internal and external strains. Among the main properties that can be calculated from the resulting Cartesian, second-derivative matrix are the vibrational frequencies, from which the phonon density of states can be obtained. From the latter, we may calculate a wide range of quantities, including the Helmholz free energy at the specified temperature. Afterward, the derivative of the Helmholz free energy with respect to the unit cell volume can be calculated numerically by finite differences.

Once the Gibbs free energy has been calculated by this procedure, the next stage of a free energy minimization is to expand or contract isotropically the unit cell until the external pressure balances the internal pressure. Having done this then the derivatives of the Gibbs free energy can be evaluated numerically by finite differences and the unit cell optimized with respect to this quantity. This whole procedure is done automatically by the GULP code. More details of the method can be found in ref 16.

Because this method is based on the quasi-harmonic approximation, it leads to inaccuracies at higher temperatures, when anharmonic effects become important; hence, we studied the MgO–MnO system only up to the temperature of 1000 K. After having minimized the Gibbs free energy of the system, we calculated the energy of mixing for the minimized structure from the lattice energy difference of the mixed system with respect to the pure oxide. We must emphasize here that all energy values reported in the subsequent tables are *energies* of mixing: our calculations refer to changes in the internal energy; but for the systems examined these can with minimal error be equated to experimentally obtained enthalpies of mixing.

3. RESULTS AND DISCUSSION

3.1. Lattice Constants of the Pure Oxides and the Mixed Crystals

First, let us consider the optimized lattice constants and bulk moduli of the pure oxides, used as a starting material

TABLE 1
Lattice Constants and Bulk Moduli of the Pure Oxides[a]

	GULP		CRYSTAL HF		CRYSTAL HF + corr		Experiment	
Oxides	a (Å)	B (GPa)	a (Å)	B (GPa)	a (Å)	B (GPa)	a (Å)	B (GPa)
MgO	4.207	239	4.203	181	4.096	188	4.213	165
CaO	4.812	136	4.847	127	4.708	150	4.8105	116
MnO	4.442	180	4.522	171	4.384	211	4.445	154
NiO	4.179	250	4.263	210	4.134	266	4.1769	190

[a] The experimental lattice constants are from ref 36. The experimental bulk modulus for MgO is from ref 37 (measured at 4 K), for CaO from ref 38 (the value is linearly extrapolated to 0 K), for MnO from ref 39 (measured at 300 K), and for NiO from ref 40 (measured at 300 K).

for the mixed crystals. In the case of MnO and NiO we present the results for the ferromagnetic state; the lattice constants for the antiferromagnetic state are very similar (11). Table 1 contains the calculated lattice constants and bulk moduli obtained with the three different Hamiltonians that we have employed: interatomic potentials (column GULP), Hartree–Fock (column HF), and Hartree–Fock with *a posteriori* correction for electron correlation (column HF + corr); in the last column we report the experimental values.

The equilibrium lattice constants of the pure oxides calculated with the atomistic simulations agree very well with the experimental values, because the experimental lattice constants of the pure oxides were used for the derivation of the interatomic potentials in the original work (18). The *ab initio* Hartree–Fock calculations overestimate the lattice parameters by about 2%, with the exception of MgO, which is well represented at the Hartree–Fock level; on the contrary, the HF results corrected for the electron correlation underestimate the lattice constants with respect to the room temperature values by ca. -1% to -2%, as found in the previous studies on these oxides (10, 19).

On the other hand, the bulk moduli of the pure oxides in the atomistic simulations are inaccurately represented—i.e. they are up to 45% too large in the case of MgO—and they are better represented by the Hartree–Fock calculations, for which they are about 10% larger than the experimental values. At the HF + corr level the deviations increase, mostly because of the smaller lattice constants. We shall discuss the influence of deviations in the calculated bulk moduli on the energies of mixing in Section 3.3.

We now examine the change in the calculated lattice constants for the three solid solutions studied. We comment briefly on the optimization procedure employed: in our HF calculations we first optimized the lattice constants of the solid solutions, keeping the oxygen sublattice in the unrelaxed cubic positions; afterward we allowed a full relaxation of the internal coordinates of the oxygen ions, leaving the lattice constant unchanged. We checked *a posteriori* that this simplified, two-step optimization procedure does not introduce major differences compared with the simultaneous relaxation of lattice constants and internal coordinates: for example, the lattice constant of the 50% mixture of MgO–MnO differs by only 0.01 Å in the two methods, while the energy of mixing decreased by only 0.1 kJ/mol when we considered the simultaneous rather than the subsequent relaxation of lattice constants and internal coordinates. Calculations for the other 50% solid solutions with both optimization methods show similar results. We checked also some of the 12.5% solid solutions and found that the two optimization procedures provide the same result for both the equilibrium lattice parameters and the energies of mixing. Furthermore, we did not optimize the angle in the rhombohedral double unit cells. Again this does not have an appreciable influence on the energies of mixing as we confirmed for two systems, where the energies of mixing decreased by less than 0.1 kJ/mol when we allowed the angle to change.

The values of the equilibrium lattice parameters for the MnO–NiO, MgO–MnO, and CaO–MnO solid solutions are plotted in Fig. 1. We note in particular that the results from both the atomistic simulations and the Hartree–Fock calculations (with and without correlation correction) show that the lattice constants of the MnO–NiO and CaO–MnO systems obey Vegard's law, as also found experimentally (20, 21). In the MgO–MnO system the atomistic simulations predict that even this system should obey Vegard's law, whereas the Hartree–Fock techniques find small positive deviations from Vegard's law. The latter result is in better agreement with the experimental evidence, which suggests that such small deviations from linearity indeed occur (21–24). However, the extent of the deviation varies between the different investigations; moreover, the study by Gripenberg *et al.* (23) could be consistent with Vegard's law if we consider the uncertainty of the experimental values.

The absolute values of the lattice parameters obtained experimentally (20, 21, 23) agree in all three mixed systems with the atomistic simulations within ca. $\pm 0.3\%$. (Because of the close agreement, the experimental parameters are not plotted in Fig. 1.) This behavior is expected, since the potentials for the pure oxides for these calculations have been fitted to the experimental (room temperature) lattice constants. The Hartree–Fock results for the mixed systems, on the other hand, reflect the errors in the calculated lattice parameters of the pure oxides. For the solid solutions, in which the error in the component oxides is uniform, as in MnO–NiO, the slope of Vegard's curve is the same as experimentally observed, and the absolute values are shifted uniformly. It is also worth noting that the correlation-corrected Hartree–Fock values are calculated at 0 K, while the reported experimental results were obtained at room

temperature, which could partly explain the small ($\sim$1%) underestimation of the lattice parameters in our quantum mechanical calculations. The CaO–MnO system is also represented reasonably well, while the HF and HF + corr calculations in the MgO–MnO system have a different slope from the experimental, because the error in the lattice parameter of the pure oxides is in this case not uniform.

We note at this point that it is important for the calculation of the energies of mixing that there are at most small deviations from Vegard's law. The mixing energy is calculated as the difference between the energy of the mixed system and that of the pure oxides, and errors arising from the slight mismatch of calculated and experimental lattice parameters affect to a very similar extent pure and mixed oxides, provided deviations from Vegard's law are small.

3.2. *Energies of Mixing of the MnO–NiO, MgO–MnO and CaO–MnO Solid Solutions*

Having described the lattice constants of the solid solutions, we turn now to the energies of mixing ΔE_{mix}, which, as argued above, we may in practice equate to experimental enthalpies. The calculated values of ΔE_{mix} were obtained as the energy difference between the energy E_{super} of the supercell $M_xM'_yO_{x+y}$ employed to represent the solid solution and the energy of the x and y unit cells of the pure oxides MO (E_{MO}) and $M'O$ ($E_{M'O}$):

$$\Delta E_{\text{mix}} = (E_{\text{super}} - xE_{MO} - yE_{M'O})/(x + y).$$

In calculating ΔE_{mix} we have used the following convention for the magnetic systems: the lattice energies of the pure oxides in the case of the antiferromagnetic/antiferrimagnetic ordering in the solid solutions are the antiferromagnetic pure oxides; when we calculate ΔE_{mix} of the ferromagnetic/ferrimagnetic solid solutions, instead, we have used the energy of the ferromagnetic pure oxides as reference.

The results of our calculations of ΔE_{mix} for the ferromagnetic/ferrimagnetic solid solutions are reported in Tables 2–4, which contain the energies of mixing from the atomistic simulations (GULP) and from the HF and HF + corr calculations with and without relaxation of the internal (oxygen) coordinates. Table 2 contains additionally the mixing energies of the antiferrimagnetic solid solutions of MnO–NiO. The magnitude of the oxygen relaxation around the metal ion M is reported in Table 5 (the nature of the metal ion, M, being shown in parentheses). Finally, plots of the calculated mixing energies and of the experimental data are shown in Figs. 2–4.

(a) MnO–NiO. The available experimental data for this system are in relatively good agreement and provide a reference system to assess the validity of our calculated energy

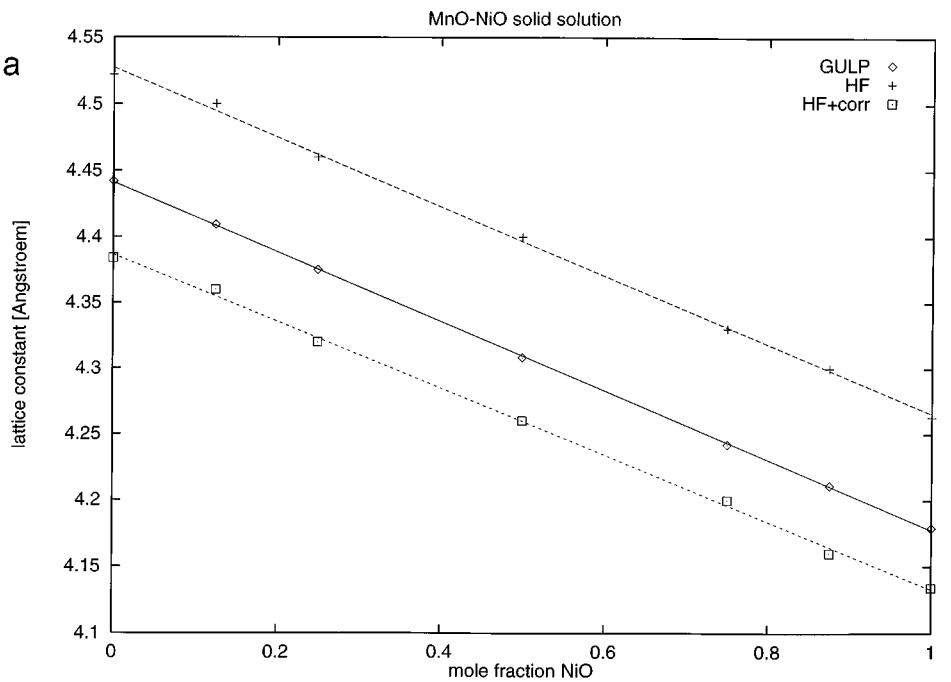

FIG. 1. Lattice constants (Å) of the MnO–NiO (a), MgO-MnO (b), and CaO–MnO (c) solid solutions: GULP = atomistic simulations; HF = Hartree–Fock calculations; HF + corr = HF with *a posteriori*–correlation correction.

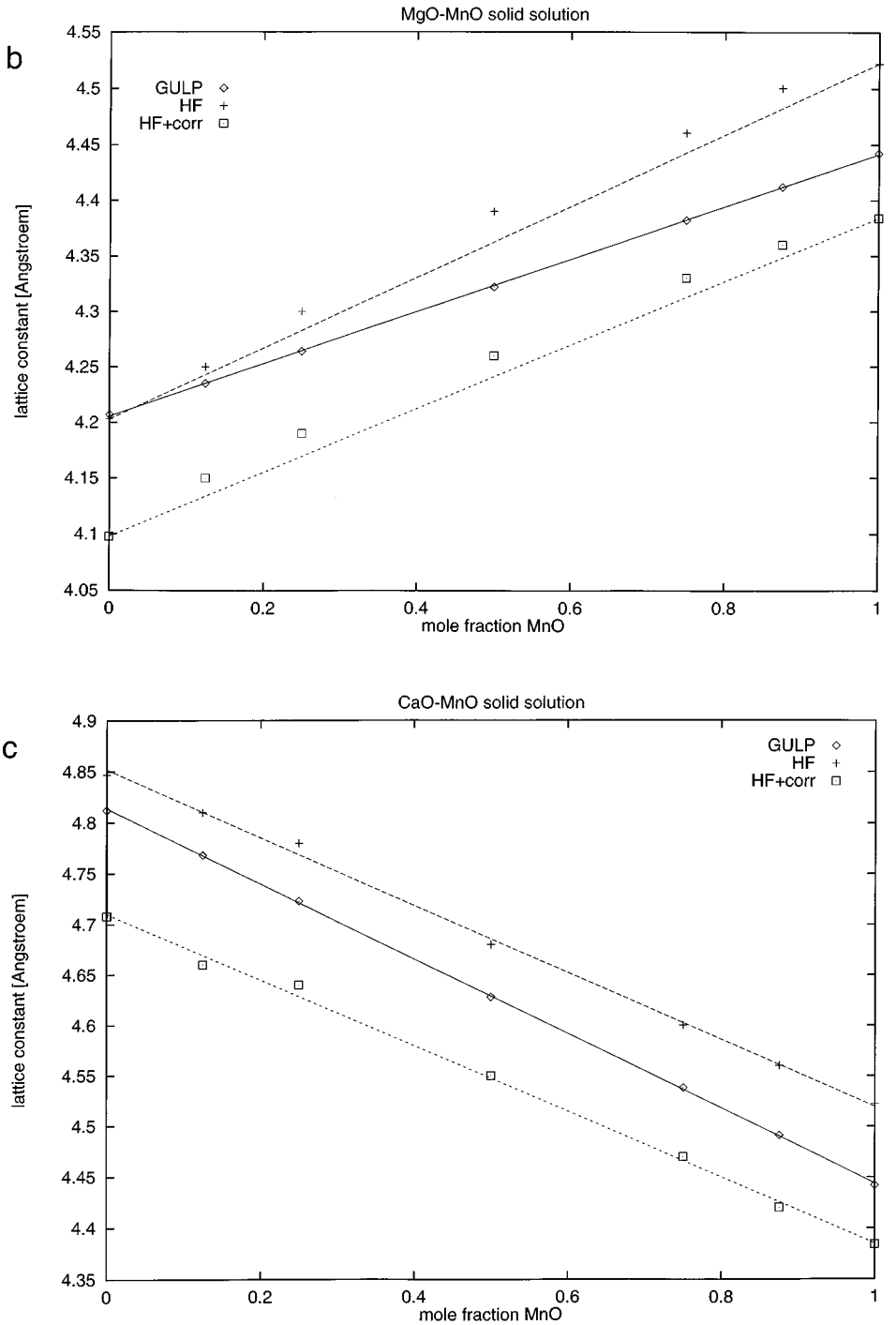

FIG. 1—*Continued*

values. We discuss first our results for the ferrimagnetic (FM) and afterward for the antiferrimagnetic (AFM) solid solutions. We recall, in fact, that the neglect of the spin ordering was one of the approximations introduced in the earlier quantum mechanical calculations on the systems MgO–MnO and MgO–NiO (6), and we aim to test whether a different magnetic ordering can cause major changes in the mixing energy.

In the FM MnO–NiO solid solutions for both our HF and HF + corr calculations, after considering a full relaxation of the internal coordinates, we find good agreement with the experimental data of Catlow *et al.* (20),

TABLE 2
Energies of Mixing (kJ/mol) of the MnO–NiO Solid Solutions: (a) HF, FM; (b) HF, AFM; (c) HF+corr, FM; (d) HF, FM; (e) HF, AFM; (f) HF+corr, FM; (g) Ref 20; (h) Ref 25[a]

		CRYSTAL Oxygen fixed			CRYSTAL Oxygen relaxed			Experiment	
MnO–NiO	GULP	a	b	c	d	e	f	g	h
12.5% NiO	3.43	3.24	3.49	3.05	2.26	2.49	2.20	1.3	1.5
25% NiO	5.59	5.86	6.10	5.44	3.48	3.76		2.2	2.5
50% NiO	6.02	6.65	6.97	6.77	3.81	4.14	2.74	2.6	3.5
75% NiO	5.79	5.27	5.50	5.63	3.33	3.71		1.6	2.5
87.5% NiO	3.61	3.03	3.37	3.09	2.06	2.43	1.82	0.9	1.5

[a]HF = Hartree–Fock, corr = correlation correction, FM = ferrimagnetic, AFM = antiferrimagnetic.

Cameron and Unger (25), and Labus and Róg (26), as evident from Fig. 2. (We note that a further experimental investigation was undertaken by Paulsson and Rosen (27), but they reported only activity values.) This agreement is particularly satisfactory, since the energy of mixing is six orders of magnitude smaller than the total energies, from which the energy of mixing was calculated: e.g., $\Delta E_{\text{mix}} = 2.74\ \text{kJ/mol} = 1.0 \times 10^{-3}$ hartree for the 50% MnO–NiO solid solutions and $E_{\text{NiO}} = 1.6 \times 10^{+3}$ hartree for the total energy of pure NiO (HF + corr calculation).

The first important conclusion that we can draw by examining the results of Table 2 is that relaxation of the internal coordinates is necessary for the correct calculation of the energies of mixing: in all the systems investigated the calculated values are up to 50% smaller due to relaxation. The absolute magnitude of the relaxation of the oxygen ions is about 0.03–0.05 Å in all the systems studied (Table 5). We also find that the inclusion of electron correlation has the effect of reducing the calculated values of the mixing energies with respect to the pure Hartree–Fock values; the importance of electron correlation is especially relevant for the 50% solid solutions. The energy values obtained from the atomistic simulations for the MnO–NiO solid solutions, instead, are too high by a factor of more than two with respect to the experimental values; we return to this point later in the discussion of Section 3.3. From the above comparison we see that the correlation-corrected Hartree–Fock results reproduce correctly the experimental data in this system and give more reliable results for the energies of mixing than do the results of the atomistic simulations.

Regarding the effects of the magnetic ordering, we would expect that the MnO–NiO solid solutions should be more stable in the AFM spin state, because the AFM ordering of spins is more stable for both the component oxides. Therefore we have checked whether performing the calculations

TABLE 3
Energies of Mixing (kJ/mol) of the MgO–MnO Solid Solutions

		CRYSTAL Oxygen fixed		CRYSTAL Oxygen relaxed		Experiment	
MgO–MnO	GULP	HF	HF+corr	HF	HF+corr	Ref 23	Ref 28[a]
12.5% MnO	2.85	6.25	5.72	4.40	3.89	2.2	1.8
25% MnO	4.57	10.48	9.70	6.82		3.9	3.0
50% MnO	4.76	11.96	10.78	6.67	5.20	5.3	4.0
75% MnO	4.43	9.00	7.96	6.51		3.0	3.6
87.5% MnO	2.71	4.68	4.23	3.66	3.20	1.6	2.1

[a] These values are estimated by Gripenberg *et al.* (23) from the activity data of Raghavan (28).

TABLE 4
Energies of Mixing (kJ/mol) of the CaO–MnO Solid Solutions

		CRYSTAL Oxygen fixed		CRYSTAL Oxygen relaxed		Experiment	
CaO–MnO	GULP	HF	HF+corr	HF	HF+corr	Ref 1	Ref 2
12.5% MnO	5.10	4.24	4.90	3.64	3.79	(1.7)	6.2
25% MnO	8.46	7.54	8.78	6.35		2.9	9.2
50% MnO	9.22	10.75	10.06	6.71	5.86	4.0	10.4
75% MnO	9.13	7.09	8.39	5.16		3.2	8.0
87.5% MnO	5.81	4.25	4.46	3.20	3.17	(1.7)	

TABLE 5
Oxygen Relaxation (Å) for the MO–M′O Solid Solutions[a]

MO–M′O	GULP	CRYSTAL HF	CRYSTAL HF + corr
MnO–NiO			
12.5% NiO	− 0.037 (Ni)	− 0.04 (Ni)	− 0.03 (Ni)
25% NiO	− 0.037 (Ni)	− 0.03 (Ni)	
50% NiO	− 0.036 (Ni)	− 0.03 (Ni)	− 0.03 (Ni)
75% NiO	0.034 (Mn)	0.03 (Mn)	
87.5% NiO	0.034 (Mn)	0.03 (Mn)	0.03 (Mn)
MgO–MnO			
12.5% MnO	0.031 (Mn)	0.04 (Mn)	0.04 (Mn)
25% MnO	0.031 (Mn)	0.04 (Mn)	
50% MnO	0.032 (Mn)	0.04 (Mn)	0.04 (Mn)
75% MnO	− 0.032 (Mg)	− 0.04 (Mg)	
87.5% MnO	− 0.033 (Mg)	− 0.04 (Mg)	− 0.03 (Mg)
CaO–MnO			
12.5% MnO	− 0.048 (Mn)	− 0.03 (Mn)	− 0.04 (Mn)
25% MnO	− 0.048 (Mn)	− 0.03 (Mn)	
50% MnO	− 0.049 (Mn)	− 0.05 (Mn)	− 0.035 (Mn)
75% MnO	0.050 (Ca)	0.03 (Ca)	
87.5% MnO	0.049 (Ca)	0.04 (Ca)	0.04 (Ca)

[a] The reported values refer to the change in the metal–oxygen distance (the metal is indicated in parentheses) between the unrelaxed and relaxed structures at the equilibrium lattice constant of each solid solution.

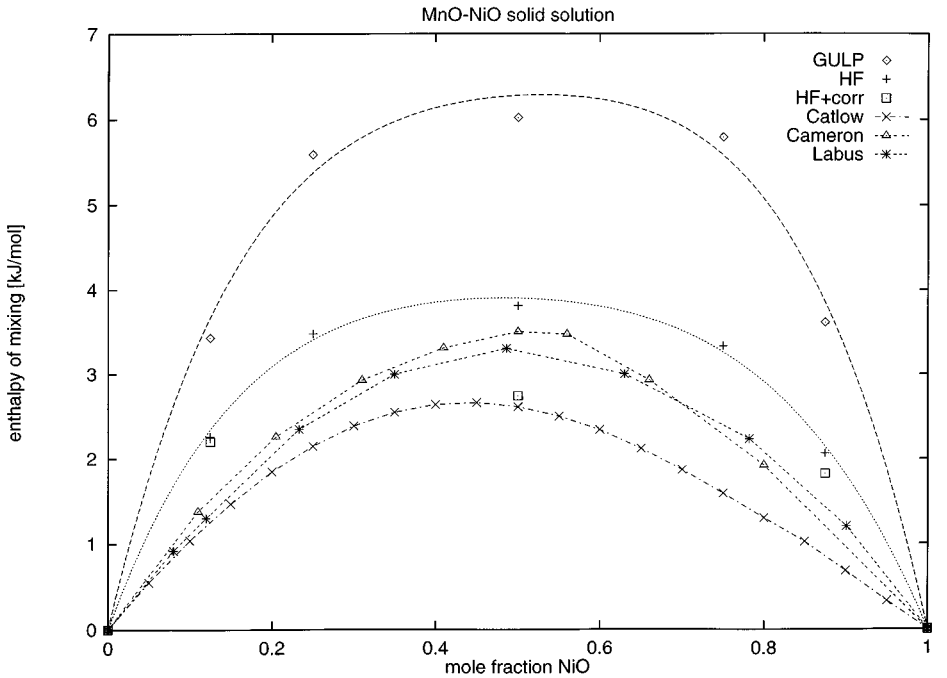

FIG. 2. Energies of mixing (kJ/mol) of the MnO–NiO solid solutions: GULP = atomistic simulations; HF = Hartree–Fock calculations, oxygen ions relaxed; HF + corr = HF with *a posteriori* electron correlation correction, oxygen ions relaxed; Catlow = experimental data from Catlow et al. (20); Cameron = Cameron and Unger (25); Labus = Labus and Róg (26).

in the AFM spin state influences significantly the calculated values of the mixing energies. As noted earlier, the spins in all the supercells for the AFM solid solutions have been aligned in ferrimagnetic (111) sheets, with adjacent sheets having antiparallel spin, which corresponds to the experimentally observed antiferromagnetic spin setting in MnO and NiO. To calculate the mixing energies of the antiferrimagnetic MnO–NiO solid solutions, we used the same geometry (lattice constants and oxygen displacements) as optimized in the corresponding ferrimagnetic state of the system. The justification for this procedure is that the calculated lattice constants of pure ferromagnetic and antiferromagnetic MnO and NiO differ by only 0.002 Å for MnO and less than 0.001 Å for NiO (11), so that we can assume that the lattice constants and oxygen displacements are independent of the spin state of the system.

The results of both FM and AFM calculations at the HF level are reported in Table 2 in columns a and b respectively for unrelaxed oxygen ions and in columns d and e for relaxed oxygen ions. We note, first, that the total energy of the AFM solid solutions is always lower than that of the corresponding FM solid solutions; we therefore confirm that the ground state electronic configuration of the mixed crystals involves the same relative orientation of spins as in the pure oxides. Considering the energetics, the data in Table 2 show that the energies of mixing calculated in the AFM crystals are slightly higher (by about 0.3 kJ/mol) than those calculated for the FM systems. This energy balance is obtained because the energy difference between the FM and AFM spin orderings is higher in the pure oxides than in the mixed crystals. It is important to note, however, that the overall description of the energies of mixing is not greatly affected by this difference (compare columns d and e of Table 2). In the following sections we therefore neglect the problem of the magnetic ordering, and for the MgO–MnO and CaO–MnO systems we perform calculations only in the computationally less expensive FM ordering of both the pure and mixed oxides. The problem is also less important in these solid solutions, because Mg^{2+} and Ca^{2+} are nonmagnetic ions and they "dilute" the Mn^{2+} spin in the solid solutions, so that the energy difference between different spin orderings is expected to decrease.

(*b*) *MgO–MnO.* There are several experimental studies of the MgO–MnO system (Gripenberg *et al.* (23), Raghavan (28), Raghavan *et al.* (29), Hahn and Muan (24), Tsai and Muan (30), and the incomplete older study of Woermann and Muan (21)). In the study of Tsai and Muan (30) the temperature dependence of the measured activities is unusual and leads to unphysical values for the mixing enthalpies and entropies (see also the comment by Wu *et al.* (4) on this investigation). The enthalpies of mixing from Hahn and Muan (24), calculated by Gripenberg *et al.* (23) from Hahn's activity data, are considerably higher in energy than the

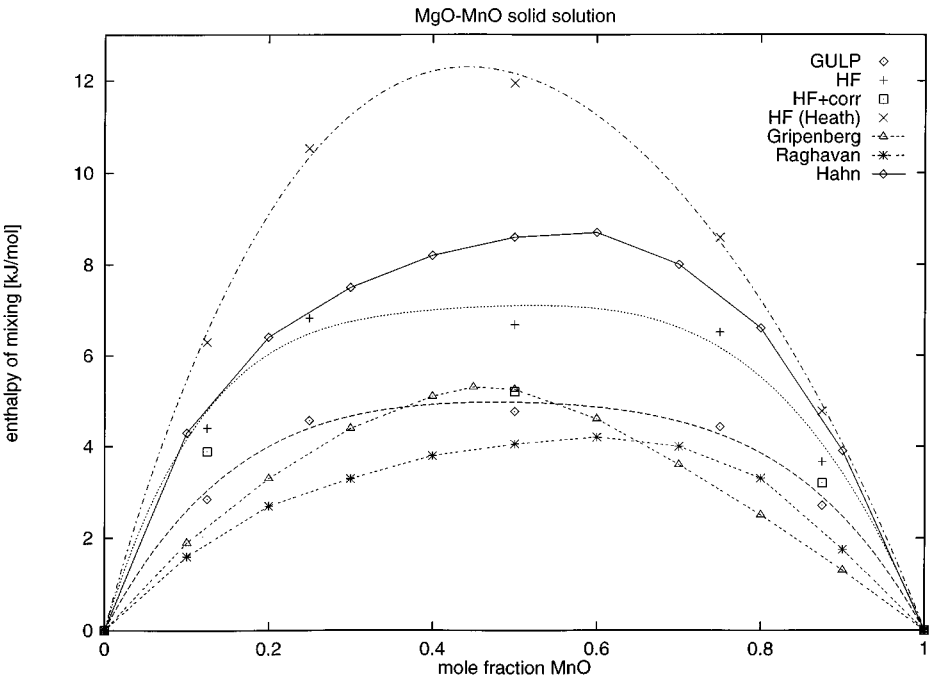

FIG. 3. Energies of mixing (kJ/mol) of the MgO–MnO solid solutions: HF (Heath) = Hartree–Fock calculations from Heath *et al.* (6); Gripenberg = experimental data from Gripenberg et al. (23); Raghavan = estimated by Gripenberg *et al.* (23) from the activity data of Raghavan (28); Hahn = estimated by Gripenberg et al. (23) from the activity data of Hahn and Muan (24); the other abbreviations are the same as in Fig. 2.

values reported by Gripenberg *et al.* (23) and Raghavan (28). In addition to the experimental values there is also the recent theoretical Hartree–Fock and atomistic simulation study by Heath *et al.* (6), which used techniques that are similar to ours, but which did not include relaxation of the internal supercell coordinates. The energy values, which arise from the unrelaxed system, as calculated in ref 6 at both the HF and the HF + corr level are even higher than the experimental values of Hahn and Muan (24). On the other hand, we have shown in the MnO–NiO system that a full account of relaxation is necessary; when relaxation is properly considered, as in our present study (Table 3 and Fig. 3), the mixing energies decrease by a factor of two. Now the HF + corr and the atomistic calculations strongly support the experimental studies of Gripenberg *et al.* (23) and Raghavan (28), while the enthalpies of Hahn and Muan (24) appear to be too high. The differences between our quantum mechanically derived mixing energies and those of Heath *et al.* are therefore due to the influence of the relaxation energy, which is not surprising, given the appreciable difference in the lattice parameters of the pure oxides MgO and MnO (see Table 1). Indeed, our energies of mixing in the unrelaxed HF and HF + corr studies are in close agreement with the values of Heath *et al.* (6), since we both used the same metal basis set in the Hartree–Fock studies; only the oxygen basis set was slightly different. Heath *et al.* (6) also calculated, in contrast to our study, high energies of mixing in their (relaxed) atomistic simulations; the value for the 50% solid solution is, for example, 7.97 kJ/mol, considerably higher than the value of 4.76 kJ/mol obtained in our atomistic study. We shall comment further on this point in the next subsection.

(*c*) *CaO–MnO.* Our results for CaO–MnO are especially interesting, because the available experimental data are very contradictory: on the one hand, there are some older incomplete measurements of (extrapolated) activities in this system (see, e.g., Brezny *et al.* (31) and Tiberg and Muan (32)) which do not give detailed information on enthalpies of mixing. On the other hand, we can find three more recent studies, which give contradictory results: Róg *et al.* (1) reported, for the 50% solid solution, a value for the mixing enthalpy of 4.0 kJ/mol; Raghavan *et al.* (2) reported 10.4 kJ/mol instead. In the third investigation of Tsai and Muan (30) the temperature dependence of their activities is very high, which leads to unphysical values for the mixing enthalpies and entropies (see again the remark by Wu *et al.* (4) on this investigation). Our HF and HF + corr calculations lie in between the study of Róg *et al.* and that of Raghavan *et al.*, although our HF + corr values, which, as we have seen earlier for the MnO–NiO system, we consider the most reliable, are closer to Róg's values. The atomistic simulations are very close to the values of Raghavan *et al.*, but as in the MnO–NiO system they are higher by a factor of about two than the HF + corr values. Recalling the unsatisfactory results for the atomistic simulations in the

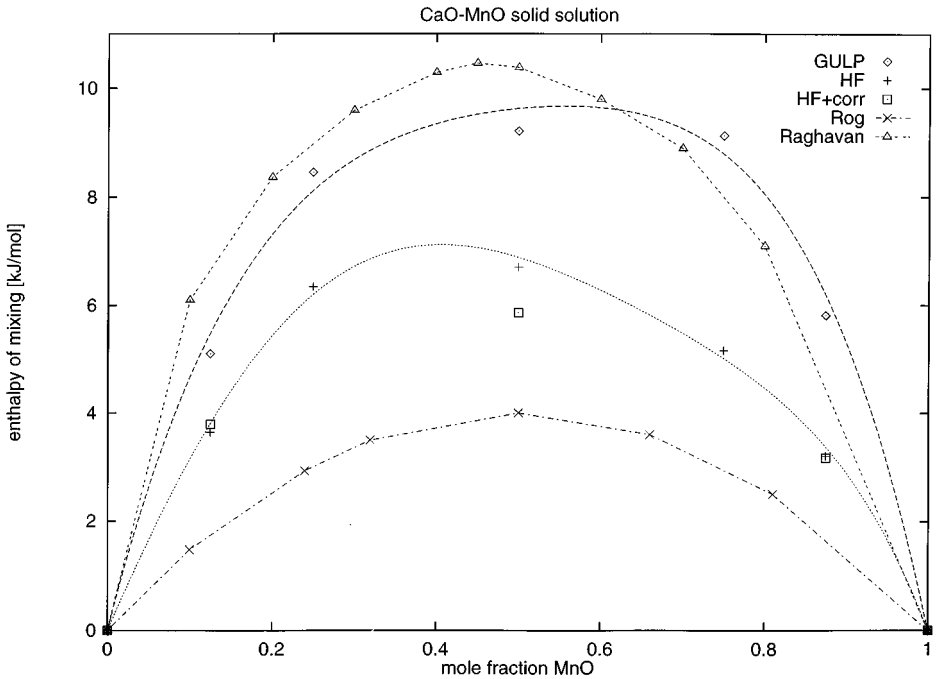

FIG. 4. Energies of mixing (kJ/mol) of the CaO–MnO solid solutions: Rog = experimental data from Róg *et al.* (1); Raghavan = Raghavan *et al.* (2); the other abbreviations are the same as in Fig. 2.

MnO–NiO system and the close agreement of the fully relaxed HF + corr values with experiment in the MnO–NiO and MgO–MnO systems and considering the simple nature of the interatomic potentials, we suggest that the results from the atomistic simulations are too high. Probably the HF + corr calculations are close to the true values. Further experiments to resolve the controversy and to determine the enthalpies of mixing should be carried out on this system.

3.3. Effect of the Interatomic Potentials on the Energies of Mixing Calculated with Atomistic Lattice Simulations

We have seen in the previous section that the energies of mixing calculated using the Hartree–Fock technique, and in particular the correlation-corrected results, are in good agreement with the available experimental data. On the other hand, we found that the atomistic simulations overestimate the mixing energies of MnO–NiO and CaO–MnO. We have also seen that Heath *et al.* (6) calculated much higher energies of mixing than ours in their atomistic simulations for MgO–MnO. To examine in greater detail the reasons for these discrepancies, we compared the results obtained with two sets of interatomic potentials available in the literature. We also derived two new sets of parameters by including the bulk modulus in the empirical observables reproduced, and by fitting to our *ab initio* results, respectively, to improve the accuracy of the atomistic values of the energies of mixing.

Let us turn to the first point and try to understand why the mixing energies calculated with interatomic potentials are overestimated with respect to the correlation-corrected Hartree–Fock results. To do this, we focus on the data reported in Table 1: as we already remarked in Section 3.1. in fact, the interatomic potentials derived by Lewis and Catlow (17, 18), which we have employed in our calculations, largely overestimate the bulk moduli of the pure oxides, as the main criterion used in deriving these potentials was the correct reproduction of the lattice parameter and the static dielectric constant. In a cubic rock salt structure changes of volume can only be obtained by changing the lattice spacing; the bulk modulus estimates therefore the resistance opposed by the material to uniform changes of the metal–oxygen distance. In our atomistic simulations, the above quantity is therefore largely overestimated with respect to the correct value, in a way proportional to the overestimation of the calculated with respect to the experimental value of the bulk modulus (45% for MgO, 32% for NiO, and 17% for CaO and MnO). In the solid solutions, by replacing one cation of the host system with another metal species with a different ionic radius, we introduce a local pressure into the structure. By examining the trend in the calculated bulk moduli, it is not surprising therefore that the reaction of the system to the strain and hence the energetics of mixing are overestimated. To test this idea we have derived two new sets of potentials. The first is obtained from the previously used potentials of Lewis and Catlow (18), but

we refitted the A and ρ parameters of the metal–oxygen Buckingham potential [$E = A\exp(-r/\rho)$], including the experimental bulk moduli in addition to the lattice constants of the pure oxides in the empirical fit. The second set of potentials has been fitted to reproduce the energy hypersurfaces of our HF + corr calculations of the pure oxides. Again, we allowed only the M–O and not the O–O parameters to change. The A and ρ parameters of the two new potentials are reported in Table 6, together with the A and ρ parameters of Lewis and Catlow. Finally, we recalculated our energies of mixing with the published empirical potentials of Stoneham and Sangster (33), which were used by Heath *et al.* (6). Results for the energies of mixing of the MnO–NiO solid solutions are reported in Table 7.

If we compare the values of the mixing energy from the three new potentials with those previously calculated, we see that the potentials of Stoneham and Sangster (33) give similar, but even higher energies of mixing than the potentials of Lewis and Catlow (18) and give therefore no improvement in the results. This is not surprising, since the two sets of potentials are fitted to similar experimental data. The potentials fitted to the experimental bulk moduli and lattice constants cause, as expected, a decrease of the mixing energy, although the calculated values are still higher than those obtained in our quantum mechanical calculations and from experimental data. We have therefore obtained the interesting result that a correct reproduction of the experimental pressure dependence of the pure constituent oxides, via the inclusion of the bulk modulus in the fitting procedure of the interatomic potentials, is important, but not sufficient to reproduce correctly the experimental energies of mixing with interatomic potentials.

The last set of potentials reported in Table 6 is that fitted to reproduce the energy hypersurfaces of the HF + corr calculations of the pure oxides. These potentials actually predict much smaller energies of mixing: the calculated values are nearly the same as the values obtained from the relaxed Hartree–Fock calculations, although the extra energy gain obtained through the correlation correction in the 50% mixture is not reproduced by the calculations based on interatomic potentials. As we have pointed out in Section 3.2, the correlation correction in the relaxed systems is much more important for the 50% than for the 12.5 and 87.5% mixtures. To understand the reason for this effect, we report, in Fig. 5, two projections of the system in the (001) plane, which show geometry and relaxation of the 12.5 and 50% solid solutions of our periodic MnO–NiO calculations. Due to the different effective size of the two cations, relaxation involves a radial movement of the oxygens in the direction from the Mn to the Ni ions. In the 12.5% solid solution the Ni cations are sufficiently separated from one another, and the oxygen relaxations around separate Ni ions do not interfere. The situation is represented in Fig. 5a; as we can see the local distortion around each Ni is symmetric and very similar to a uniform change of the lattice spacing in pure NiO; it is therefore correctly represented by a potential that reproduces the bulk modulus of the material. In the 50% solid solution the situation is changed: in a model of the solid solution based on periodic boundary conditions, the solid is characterized by a long-range order imposed by the unit-cell periodicity. In the relative disposition of the two cations that we have chosen, each metal occupies alternate (111) planes. As evident from Fig. 5b, the oxygen relaxations around each Ni ion do in this case interfere, and the net movement contains an appreciable component in the O–O and not only the O–Ni direction. We have not included explicitly the former component in the derivation of our potentials, where we retained the original parameters for the O–O interaction as derived in the work of Catlow (17). The O relaxation represented in Fig. 5b is no longer radial and contains components of the individual elastic constants of the materials; a correct value of the bulk modulus of the pure oxides does not therefore guarantee that the energetics of this relaxation is correctly reproduced.

Figure 5b can also provide an explanation for the more pronounced importance of electronic correlation in the 50% mixtures, which we highlighted in our discussion of the quantum mechanical results: in this case relaxation changes

TABLE 6
Atomistic Buckingham M–O potentials [$E = A\exp(-r/\rho)$] Fitted to the Experimental Bulk Moduli and Lattice Constants of the Pure Oxides (Potential 1) and to the Energy Surface of the HF+corr Calculations of the Pure Oxides (Potential 2)

	Lewis–Catlow potential (18)		Potential 1		Potential 2	
MO	A (eV)	ρ (Å)	A (eV)	ρ (Å)	A (eV)	ρ (Å)
MgO	1428.5	0.2945	323.42	0.3885	299.13	0.3868
CaO	1090.4	0.3437	546.49	0.3879	651.93	0.3692
MnO	1007.4	0.3262	524.68	0.3671	253.87	0.4216
NiO	1582.5	0.2882	485.64	0.3549	363.12	0.3747

TABLE 7
Energies of Mixing (kJ/mol) of the MnO–NiO Solid Solutions Obtained with Different Atomistic Potentials[a]

MnO–NiO	Lewis–Catlow potential (18)	Stoneham–Sangster potential (33)	Potential 1	Potential 2	HF + corr
12.5% NiO	3.43	4.07	2.91	2.14	2.20
25% NiO	5.59	6.63	4.83	3.58	
50% NiO	6.02	7.11	5.48	4.33	2.74
75% NiO	5.79	6.83	5.13	3.65	
87.5% NiO	3.61	4.25	3.20	2.20	1.82

[a] The parameters of potentials 1 and 2 are those from Table 6.

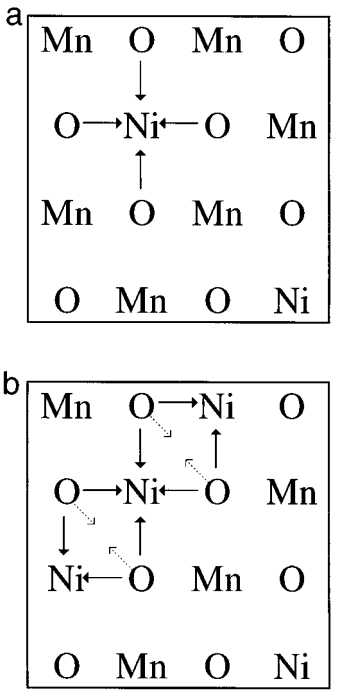

FIG. 5. Schematic representation of the solid solution of 12.5% NiO in MnO (a) and 50% NiO in MnO (b). The plots are drawn in the (001) plane of the materials. The arrows indicate the oxygen relaxation around the metal. The dotted arrows in (b) show the overall movement of the oxygens when they relax toward the two nickel ions.

the inter-oxygen spacing. Since the anions are polarizable species, we expect the effect of correlation to be much more important in the O–O than in the O–M interaction, thus explaining the extra stabilization of the solid solution due to correlation. The fact that the energies of mixing for the unrelaxed systems do not show the extra energy gain due to correlation (see for instance Table 2 for the 50% MnO–NiO solid solution, in which the mixing energy in the HF + corr calculations is higher than in the pure HF level) gives further evidence for our explanation.

The previous analysis also suggests that it is obviously possible to improve the description of the energies of mixing with atomistic simulations, but we must in this case include explicit information about anisotropic deformations of the system when fitting the interatomic potentials. In this respect we note that in rock salt materials, described with central force potentials, the Cauchy relation applies, which requires that the elastic constant C_{12} is equal to C_{44}, as discussed in ref 18. The discrepancy of the results of the atomistic calculations with experiment seems therefore, at least partially, linked to limitations of the potential model employed. For this reason we have not further investigated the problem. Improved interatomic potential models are currently being investigated; the extensive study of Leslie (34) on MgO, in which he was able to reproduce correctly all the elastic constants of the material, is a good example. Further detailed investigations of the mixing energies will be undertaken when improved potential models are available.

We now compare our results for the MgO–MnO solid solution with those of Heath *et al.* (6) and examine why the latter paper presents higher values than ours for the atomistic simulations of the mixing energy. First we repeated our calculations with the potentials of Sangster and Stoneham (33), as used in ref 6. The values that we obtain are reported in the column "Stoneham potential" of Table 8; they are not substantially different from the results we obtained previously using the potentials derived by Lewis and Catlow (18). Therefore, especially for the 50% solid solution, our calculated mixing energy is considerably lower than the value reported by Heath *et al.* (6). As we have seen in Section 3.2, only the neglect of relaxation can cause a major change in the calculated mixing energy. We have therefore repeated the calculations, but we excluded this time the relaxation of the internal coordinates; the energies of mixing, obtained in this way, are reported in the column "coordinates unrelaxed" of Table 8. The agreement of the 25, 75, and 50% solid solutions with the results in ref 6 is now much improved. It is important to mention at this point that the choice of the supercell to represent the solid solution is crucial. In some unit cell expansions, as in the 8-ion MM'_3O_4 (25 and 75% solid solutions) and $M_2M'_2O_4$ (50% solid solutions) supercells, all the ions are on symmetry-unique positions and no relaxation is possible. The energies of mixing for the 25, 75, and 50% solid solutions, when we do not relax the internal coordinates, are in fact very similar to the values of Heath *et al.* (6). On the other hand, the values for the 12.5 and 87.5% solid solutions agree with Heath's values when we relax the internal coordinates, since the 16-ion unit cell MM'_7O_8, which was also used in ref 6, does allow the relaxation of internal coordinates. (The small

TABLE 8
Energies of Mixing (kJ/mol) of the MgO–MnO Solid Solutions Calculated by Atomistic Simulations

MgO–MnO	Heath et al. (0 K)	Stoneham potential	Coordinates unrelaxed[a]	0 K[b]	500 K[b]	1000 K[b]
12.5% MnO	2.61	2.80	3.77	2.85	2.85	2.84
25% MnO	6.22	4.49	6.38	4.57	4.57	4.55
50% MnO	7.97	4.64	8.28	4.76	4.76	4.69
75% MnO	5.83	4.33	6.06	4.43	4.44	4.48
87.5% MnO	2.49	2.65	3.49	2.71	2.72	2.80

[a] The values reported in this column are also calculated using the Stoneham–Sangster potentials (33), but without relaxation of the internal coordinates.

[b] Gibbs free energy minimizations (including vibrational entropy and zero-point energy contributions) at the temperatures 0, 500, and 1000 K; the reported energies of mixing refer to the minimized structure. The potentials of Lewis and Catlow (18) are used.

remaining differences of about 0.2 kJ/mol may be caused by using different cutoffs for the interatomic potentials or by different numerical approximations.)

Heath *et al.* (6) also calculated the temperature dependence of the mixing energies and found an appreciable increase in the range from 0 to 1000 K. Because of the discrepancy of the static values of the mixing energies between our work and their work, we have reexamined the temperature dependence of the energy of mixing. To this purpose we have first minimized the Gibbs free energy of the system at the temperatures 0, 500, and 1000 K and afterward calculated the energy of mixing from the lattice energy difference of the mixed system with respect to the minimized pure oxide at the specified temperature. The temperature dependence of the mixing energy calculated in this way (last three colums in Table 8) is lower than that reported in ref 6. For example, for the 12.5% solid solution Heath *et al.* reported an increase of the mixing energy of more than 1.3 kJ/mol when increasing the temperature from 0 to 1000 K, while the change is almost negligible in our calculations: by calculating the mixing energies at the different temperatures via the minimization of the Gibbs free energy and using the potentials of Lewis and Catlow (18), we found a maximum change in the values of the energies of mixing of only 0.1 kJ/mol.

3.4. Electronic Structure of the Mixed Crystals

In this section we comment briefly on the electronic structure of the mixed crystals. In an earlier atomistic simulation study of the heat of solution in the MnO–NiO system, a similar discrepancy between calculated and experimental data was found, as in our atomistic simulation study. Catlow *et al.* (20) speculated that the difference could be due to a partial delocalization of one Mn^{2+} e_g electron to the conduction band of the system, leading to the formation of Mn^{3+} ions in the mixed crystals. We have investigated this hypothesis by examining the ground state electronic distribution of the solid solutions, as derived from our quantum mechanical HF calculations. In the pure magnetic oxides MnO and NiO the valence d electrons are well localized on the metal and the environment of the oxygen ions is isotropic. In contrast, the environment in the mixed oxides is no longer isotropic. As discussed earlier, the different effective size of the cations causes a geometric relaxation of the oxygen ions from the perfect lattice sites. We now investigate whether the asymmetric environment causes also an electronic relaxation of the oxygen ions of the kind suggested in ref 20. In Fig. 6 we report the spin density maps, that is the difference between the density of α and β electrons, for the pure ferromagnetic oxides and three of the ferrimagnetic MnO–NiO mixtures. It is evident from Fig. 6 that the spin density maps of the mixtures are not substantially different from those of the pure oxides and that the unpaired electrons are still localized on the metal. In other words, in the mixed crystals there is no appreciable electronic relaxation (due to the different sizes of the surrounding cations) nor any induced spin polarization (due to the asymmetric magnetic environment) on the oxygen ions. Further evidence for the absence of charge transfer and the localized electron behavior in the mixed crystals can be obtained from the density of states and from the Mulliken population analysis, which indicates virtually the same number of α–β electrons of $+4.92 \pm 0.03$ |e| for Mn and $+1.93 \pm 0.02$ |e| for Ni (and 0.00 ± 0.01 |e| for Mg and Ca) for all the different mixtures which we have examined.

On the basis of the previous analysis we can therefore exclude the possibility that the MnO–NiO solid solutions contain any Mn^{3+}; we also confirm that these are highly ionic oxides with no spin transfer to the oxygen ions due to covalent interactions and with the d electrons localized on the metal cations. This result is in agreement with a previous study reported by Towler *et al.* (35) for the $M_xMg_{1-x}O$ (M = Mn, Ni) solid solutions.

4. CONCLUSIONS

This study has considerably amplified our understanding of the structural and thermodynamic properties of mixed transition metal oxides. The major findings are as follows:

(i) The agreement of the Hartree–Fock energy values, especially those corrected *a posteriori* for electron correlation, with at least one of the available experimental data sets is usually very good. Hartree–Fock calculations are therefore an alternative route that can be used to determine energies of mixing, especially when experimental mixing enthalpies are difficult to measure or the available experimental data are in disagreement.

(ii) Our calculations predict correctly that the antiferrimagnetic ordering of cations in the system MnO–NiO is more stable than the ferrimagnetic ordering; neglecting the magnetic ordering does not, however, influence heavily the calculated mixing energy.

(iii) Atomic relaxation plays an important role in the energetics of mixing and must be properly accounted for.

(iv) The solid solutions are strongly ionic oxides with no spin transfer to the oxygen ions due to covalent interactions and with localized d electrons on the metal cations.

Additionally, we found that atomistic simulations in the case of the MnO–NiO and CaO–MnO solid solutions predict energies of mixing that are significantly too high: by fitting the interatomic potential parameters to our *ab initio* data, we were able to derive a new set of potentials which reproduce experimental results better than those previously published. Atomistic simulations are highly sensitive to the interatomic potential parameters used. However, we have shown that the discrepancy can be due to limitations of the

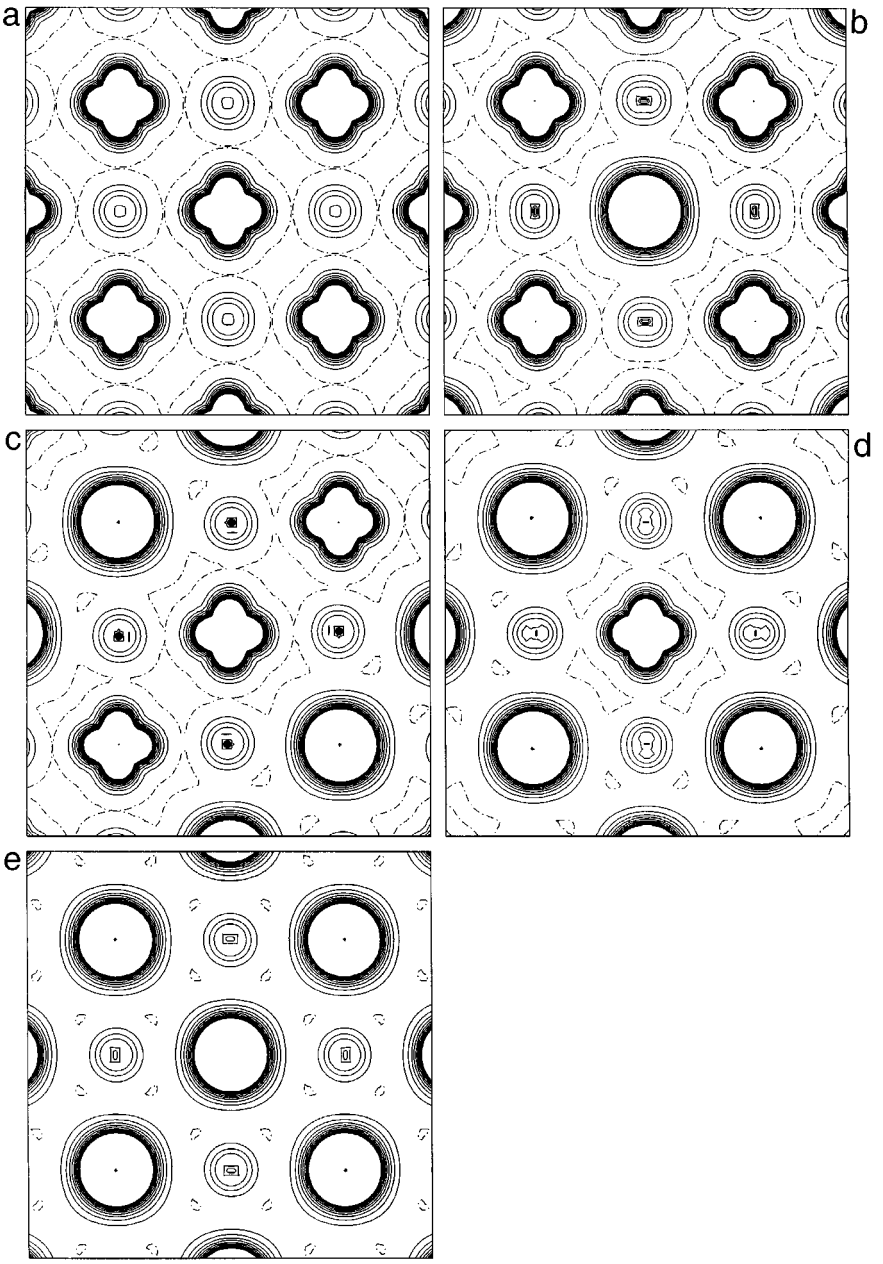

FIG. 6. Spin density maps for ferromagnetic NiO (a) and MnO (e) and for the relaxed ferrimagnetic 12.5% (b), 50% (c), and 87.5% (d) mixtures of NiO in MnO. The plots are drawn in the (001) plane of the materials. Isodensity lines are plotted from -0.1 to 0.1 au at intervals of 0.01 au (e/bohr^3). Continuous, dashed, and dotted–dashed lines correspond to positive, negative, and zero values, respectively.

model and that carefully parameterized potentials can yield more accurate results.

Finally, we calculated the temperature dependence of the energy of mixing for MgO–MnO by performing Gibbs free energy minimizations at different temperatures up to 1000 K. The results indicate a negligible temperature dependence of the energy of mixing.

ACKNOWLEDGMENTS

M.K. thanks the DFG (Deutsche Forschungsgemeinschaft) for the financial support. We are grateful to CLRC for allowing us to use the SP2 parallel computer at Daresbury Laboratory for some of our calculations. We also thank M. Leslie for useful discussions. EPSRC is thanked for the provision of computer resources at the Royal Institution.

REFERENCES

1. G. Róg, A. Kozlowska-Róg, W. Pycior, and K. Zakula, *J. Solid State Chem.* **100,** 115 (1992).
2. S. Raghavan, G. N. K. Iyengar, and K. P. Abraham, *Trans. Indian Inst. Met.* **33,** 51 (1980).
3. P. K. Davies and A. Navrotsky, *J. Solid State Chem.* **46,** 1 (1983).
4. P. Wu, G. Eriksson, and A. D. Pelton, *J. Am. Ceram. Soc.* **76,** 2065 (1993).
5. J. K. Burdett and C. Nguyen, *Chem. Mater.* **5,** 1775 (1993).
6. K. D. Heath, W. C. Mackrodt, V. R. Saunders, and M. Causà, *J. Mater. Chem.* **4,** 825 (1994).
7. R. Dovesi, V. R. Saunders, C. Roetti, M. Causà, N. M. Harrison, R. Orlando, and E. Aprà, "CRYSTAL95 User's Manual," University of Torino, Torino, 1996.
8. C. Pisani, R. Dovesi, and C. Roetti, "Hartree–Fock ab initio Treatment of Crystalline Systems" (Lecture Notes in Chemistry, Vol. 48). Springer-Verlag, Heidelberg, 1988.
9. M. I. McCarthy and N. M. Harrison, *Phys. Rev. B* **49,** 8574 (1994); R. Dovesi, C. Roetti, C. Freyria-Fava, E. Aprà V. R. Saunders, and N. M. Harrison, *Philos. Trans. R. Soc. London, Ser. A* **341,** 203 (1992).
10. C. Freyria-Fava, R. Dovesi, V. R. Saunders, M. Leslie, and C. Roetti, *J. Phys.: Condens. Matter.* **5,** 4793 (1993).
11. M. D. Towler, N. L. Allan, N. M. Harrison, V. R. Saunders, W. C. Mackrodt, and E. Aprà, *Phys. Rev. B* **50,** 5041 (1994).
12. J. P. Perdew, "Electronic Structure of Solids" (P. Ziesche and H. Eschrig, Eds.). Akademie Verlag, Berlin, 1991.
13. J. P. Perdew, J. A. Chevary, S. H. Vosko, K. A. Jackson, M. R. Pederson, D. J. Singh, and C. Fiolhais, *Phys. Rev. B* **46,** 6671 (1992).
14. "Computer Simulation in Solids" (Lecture Notes in Physics, Vol. 166) (C. R. A. Catlow and W. C. Mackrodt, Eds.). Springer-Verlag, Heidelberg, 1982.
15. J. D. Gale, *J. Chem. Soc., Faraday Trans.* **93,** 629 (1997).
16. J. D. Gale, "GULP User's Manual," Imperial College, 1997.
17. C. R. A. Catlow, *Proc. R. Soc. London, Ser. A* **353,** 533 (1977).
18. G. V. Lewis and C. R. A. Catlow, *J. Phys. C: Solid State Phys.* **18,** 1149 (1985) (potentials from Table 4, p. 1155).
19. M. I. McCarthy and N. M. Harrison, *Phys. Rev. B* **49,** 8574 (1994).
20. C. R. A. Catlow, B. E. F. Fender, and P. J. Hampson, *J. Chem. Soc., Faraday Trans. 2* **73,** 911 (1977).
21. E. Woermann and A. Muan, *Mater. Res. Bull.* **5,** 779 (1970).
22. H. Schenck, M. G. Frohberg, and R. Nünninghoff, *Arch. Eisenhüttenwes.* **35,** 269 (1964).
23. H. Gripenberg, S. Seetharaman, and L.-I. Staffansson, *Chem. Scr.* **13,** 162 (1978–1979).
24. W. C. Hahn, Jr. and A. Muan, *Mater. Res. Bull.* **5,** 955 (1970).
25. D. J. Cameron and A. E. Unger, *Metall. Trans.* **1,** 2615 (1970).
26. S. Labus and G. Róg, *Roczn. Chem.* **49,** 339 (1975).
27. H. Paulsson and E. Rosén, *Chem. Scr.* **11,** 204 (1977).
28. S. Raghavan, Ph.D. Thesis, Indian Institute of Science, Bangalore, India, 1977.
29. S. Raghavan, G. N. K. Iyengar, and K. P. Abraham, *J. Chem. Thermodyn.* **17,** 585 (1985).
30. H.-T. T. Tsai and A. Muan, *J. Am. Ceram. Soc.* **75,** 1472 (1992).
31. B. Brezny, W. R. Ryall, and A. Muan, *Mater. Res. Bull.* **5,** 481 (1970).
32. N. Tiberg and A. Muan, *Metall. Trans.* **1,** 435 (1970).
33. A. M. Stoneham and M. J. L. Sangster, *Philos. Mag. B* **52,** 717 (1985).
34. M. Leslie, private communication.
35. M. D. Towler, N. L. Allan, N. M. Harrison, V. R. Saunders, and W. C. Mackrodt, *J. Phys.: Condens. Matter* **7,** 6231 (1995).
36. A. R. West "Solid State Chemistry and Its Applications." John Wiley & Sons, New York, 1989.
37. K. Marklund and S. A. Mahmound, *Phys. Scr.* **3,** 75 (1971).
38. Z. P. Chang and E. K. Graham, *J. Phys. Chem. Solids* **28,** 1355 (1977).
39. D. W. Oliver, *J. Appl. Phys.* **40,** 893 (1969).
40. M. R. Notis, R. M. Spriggs, and W. C. Hahn, *J. Geophys. Rev.* **76,** 7052 (1971).